A Bounded Model of the Communication Delay for System Integrity Protection Schemes

Can Huang, *Student Member, IEEE*, Fangxing Li, *Senior Member, IEEE*, Tao Ding, *Member, IEEE*, Yuming Jiang, *Senior Member, IEEE*, Jiahui Guo, *Student Member, IEEE*, and Yilu Liu, *Fellow, IEEE*

***Abstract*—This paper investigates the latency of system integrity protection schemes (SIPSs) and proposes a bounded model of the communication delay. To be specific, SIPSs can be divided into wide-area protection and substation-area protection. For the former, the data buffering of phasor data concentrators and the automatic protection switching of synchronous optical network/synchronous digital hierarchy are utilized to limit the latency of regional and backbone networks, respectively; then, the communication delay is modeled as bounded, instead of average or stochastic in the literature. For the latter, the network calculus theory is used to restrict the latency in switched Ethernet networks, and the communication delay is modeled as bounded. In practice, SIPSs need to preprogram the time delay of protective relays and expect the communication delay as predictable or predetermined. Hence, the proposed bounded model is more realistic than the average or stochastic model. Further, the bounded model suggests the network dynamics and worst-case performances. It can be a useful tool in the relay setting as well as in the planning, design, and assessment of SIPS networks.**

***Index Terms*—Communication delay, IEC 61850, network calculus, system integrity protection scheme (SIPS), wide-area measurement system (WAMS).**

NOMENCLATURE

t_{delay}	Total end-to-end delay.
t_d	Communication delay.
t_{PMU}	PMU processing delay.
t_{PDC}	PDC processing delay.
t_{RN}	Regional network delay
t_{BN}	Backbone network delay.
t_{APP}	Application processing delay.
t_{wait}	PDC wait time or relative wait time.
t_{cal}	PDC calculated time.
t_{proc}	PDC additional processing time.
t_{APS}	SONET automatic switching time.
t_{SONET1}	SONET delay in the normal state.
t_{SONET2}	SONET delay in the protection state.
t_{que}	Queuing delay.
t_{prop}	Propagation delay.
t_{trans}	Transmission delay.
D_{RN}	Physical distance of regional networks.
D_{BN}	Physical distance of backbone networks.
v	Light speed in optical fibers.
L_{PMU}	PMU package length.
B	Link bandwidth.
N_{PDC}	Number of PDCs.
k	The index of PDCs.
i	The index of priority levels.
j	The index of servers.
p	The index of paths.
$\alpha(t)$	Arrival curve.
$\beta(t)$	Service curve.
r	Average traffic rate.
b	Maximum instantaneous burst.
C	Switch port rate.
R	Minimum service rate of a data flow.
θ	Latency parameter.
$\tau_{\max}$	Delay bound.
$Q_{\max}$	Backlog bound.
L^{GS}, L^{SV}	Maximum message length of GOOSE or SV.
f^{GS}, f^{SV}	Frequency of generating GOOSE or SV.

Manuscript received July 01, 2015; revised October 30, 2015; accepted January 20, 2016. Date of publication February 19, 2016; date of current version July 21, 2016. This work was supported in part by CURENT, a NSF/DOE Engineering Research Center (ERC) Program under National Science Foundation Award EEC-1041877. Paper no. TPWRD-00850-2015.

C. Huang, F. Li, J. Guo, and Y. Liu are with the Department of Electrical Engineering and Computer Science, the University of Tennessee, Knoxville, TN 37996 USA (e-mail: fli6@utk.edu).

T. Ding is with the State Key Laboratory of Electrical Insulation and Power Equipment, School of Electrical Engineering, Xi'an Jiaotong University, Xi'an, Shaanxi 710049, China.

Y. Jiang is with the Department of Telematics, Norwegian University of Science and Technology, Trondheim 7491, Norway.

Color versions of one or more of the figures in this paper are available online at http://ieeexplore.ieee.org.

Digital Object Identifier 10.1109/TPWRD.2016.2528281

I. INTRODUCTION

POWER system protection has been continuously developed since its invention in the early 1900's [1]. Protective relays, as a major component of power system protection, evolved in the last century from electromechanical relays to microprocessor relays. The supporting protection schemes were conventionally designed to isolate faulted components, so as to ensure the safety of humans and power apparatus and the stable operation of power grids [1]–[3]. Those protection schemes use local measurements only and can detect and clear local faults efficiently, while they may perform poorly under system-wide disturbances, e.g., the August 14th blackout in North America [4]. It is reported that from 1996 to 2001, the protection malfunction contributed to the initiation or evolution of about 70% of major system-wide disturbances in North America [5]. Accordingly, several new protection schemes have been proposed in the last two decades, such as the special protection scheme (SPS), remedial action scheme (RAS), and system integrity protection scheme (SIPS) [6]–[12].

The SPS is designed to detect abnormal or predetermined system conditions and take corrective actions other than or in

addition to the isolation of faulted components to maintain system reliability [6]. The SPS is also called the RAS on certain occasions and gradually expanded into the SIPS. The SIPS encompasses the SPS, the RAS, and additional schemes like under-frequency/under-voltage load shedding and out-of-step relaying, and is developed to protect the integrity of a power system or a strategic part of it [7]. The SIPS extends the protection scope from local areas to system-wide areas, which overcomes the inherent defect of conventional protection schemes [7]–[10]. On the other hand, the advancement of power system measurement and information technologies, especially wide-area measurement systems (WAMSs) provides an opportunity to implement the SIPS and enhance the performance of power system protection [11], [12].

The SIPS uses local and/or wide-area measurements for decision making, and thus needs reliable and fast communication networks. Unfortunately, practical communication networks will induce data loss and latency due to unintentional factors (e.g., human errors, equipment malfunctions and communication infrastructure limits) or intentional cyber-attacks [13]–[15]. These issues will lower the data quality and even impact the performance of SIPSs. Thus, much effort in academia and industry has been devoted to high-performance communication networks. For wide-area protection, several novel communication architecture [16], [17], medium [18], and protocols [9], [10] are developed to improve the communication infrastructure. For local protection, the quality-of-service (QoS) of communication networks is mainly guaranteed with advanced equipment and design, such as gigabit Ethernet switches, IEEE 802.1Q based virtual local area network (VLAN), and IEC 62439 based redundant design [19], [20]. These methods can enhance the communication network's capacity and lower the data-loss rate, but cannot eliminate the latency.

Previous works primarily deal with the latency through experiments, simulation, or theoretical analysis. For instance, the latency of a real WAMS is measured in [21], and the communication delay is modeled as constant. The latency of a process bus network of a substation is tested in a laboratory environment in [22], and the impact of data loss and latency on digital protection is analyzed. In addition, references [19], [23]–[30] find out the latency using simulation, and the communication delay is modeled as stochastic in [23] and [24]. Reference [31] calculates the time delay through the timing diagram based theoretical analysis and determines the worst-case communication delay of the switched Ethernet. The experimental and simulation results are realistic in short-term (e.g., a few seconds or a few minutes) and under specific conditions, while in long term (e.g., a few hours to even a few days) and dynamic conditions they may be idealistic and even questionable.

In practice, prior to detection, decision, and action, SIPSs need to preprogram the time delay of protective relays and expect the data latency to be predictable or predetermined. Also, SIPSs are time-critical and reliability-oriented, so the idealistic parameters are generally unfavorable in the design of SIPSs. Hence, this work investigates the latency of SIPSs and proposes a bounded model of the communication delay. Specifically, the system integrity protection with different protection scopes is divided into wide-area protection and substation-area protection. A brief description is given as follows.

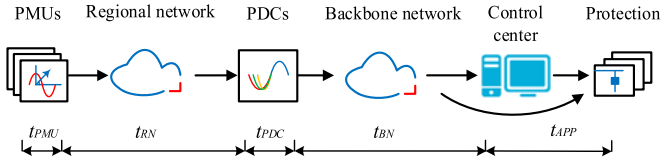

Fig. 1. Block diagram of a typical wide-area protection system.

1) Wide-area protection makes use of phasor measurement units (PMUs) based synchronized measurements and protects power systems against system-wide disturbances. The communication delay over regional and backbone networks is limited by the data buffering of phasor data concentrators (PDCs) and the automatic switching of synchronous optical network/synchronous digital hierarchy (SONET/SDH), respectively. As a result, the communication delay is modeled as bounded. When compared with the empirical or stochastic model in the literature, the bounded model is more realistic for protective devices. Moreover, the bounded model is derived from the existing WAMS and requires no additional hardware.

2) Substation-area protection is primarily referred to as the protection in a substation or between substations. Conventional protection receives analog signals via point-to-point connected electric cables and ignores communication delays. In contrast, digital protection in accordance with IEC 61850 is time critical, and it transmits analog/digital signals through optical fibers and Ethernet switches. Here, the communication delay of digital protection is analyzed and further modeled as bounded using network calculus. The network calculus theory focuses on performance guarantees, instead of the classical queuing theory dealing with average values. Hence, the bounded communication delay not only guarantees the real-time communication of digital protection, but plays an important role in the design and assessment of substation networks.

The rest of this paper is organized as follows. Sections II and III investigate the time-critical system integrity protection and propose the bounded model of the communication delay for wide-area protection and substation-area protection, respectively. Section IV presents the case studies of the IEC 61850 T2-2 substation system, the IEEE 14-bus system and the China Southern Power Grid SDH system, respectively. Finally, the conclusion and future work are drawn in Section V.

II. Communication Delays of Wide-Area Protection

A. Wide-Area Protection

Wide-area protection takes advantage of WAMS techniques and provides comprehensive protection over wide geographical areas of interconnected power systems. A wide-area protection system primarily consists of PMUs, PDCs, protective devices, a control center (CC), and regional and backbone networks as shown in Fig. 1.

In general, PMUs measure a power system's voltage and current phasors using a common time signal from the global

positioning satellite (GPS). PDCs sort various PMU data based on GPS time-tags and forward the synchrophasor data to a control center and/or protection applications. Then, protection applications can observe the power system in real-time and over wide areas, and can then take advantageous actions by an adaptive agent or expert system [32].

Obviously, the communication delay needs to be considered in wide-area protection. IEEE Std. C37.118.2 clarifies that the total delay of synchrophasor data is composed of a communication delay t_d and terminal processing delays t_{PMU} and t_{APP}, and provides their typical ranges. Also, some literatures further divide the total delay into six terms as (1) [21], [24].

$$\begin{aligned} t_{delay} &= t_{PMU} + t_d + t_{APP} \\ &= t_{PMU} + (t_{PDC} + t_{RN} + t_{BN}) + t_{APP} \\ &= t_{PMU} + (t_{PDC} + t_{prop} + t_{que} + t_{trans}) + t_{APP} \end{aligned} \tag{1}$$

where t_{PMU}, t_{PDC}, and t_{APP} are the processing delays of a PMU, a PDC, and a protection application, respectively. t_{RN} and t_{BN} are the communication delays over regional and backbone networks. Specifically, the transmission delay $t_{trans} = L_{PMU}/B$ is calculated by the PMU package length L_{PMU} (bit) and the link bandwidth B (bit/s), the propagation delay $t_{prop} = D/v$ is calculated by the distance D between nodes and the light speed v in the particular communication medium (e.g., $v \doteq 2.0 \times 10^5$ km/s in optical fibers), and the queuing delay t_{que} is determined by the traffic behavior of communication networks.

In practice, the terminal processing delays can be limited to small ranges or even fixed to constants, but the communication delay is normally uncertain and stochastic [15]. For that, the majority of previous works study the communication delay through experiments or simulations and model it with average or stochastic values [21]–[25]. For instance, Zhang *et al.* measure the communication delay of Guizhou Power Grid in 100 seconds and model the communication delay as constant [21].

As aforementioned, the experimental or simulation results may be partially true or idealistic when they are compared with the real-time values under various conditions. This work takes advantage of the low-cost and GPS-synchronized wide-area frequency measurement network (FNET) [33]–[35] and tests the communication delay of FNET in one week as shown in Figs. 2 and 3. FNET implies some nature of wide-area communications. It is observed that the communication delay may vary dramatically in the short term (e.g., one minute), and its probability distribution changes with time periods and locations. Further, a system-wide disturbance may lead to heavy traffic over communication networks, since a number of commands and alarm signals emerge instantaneously [36]–[38]. The dynamic characteristic of communication delays needs to be taken into account.

B. Modeling of Communication Delays

This work proposes a bounded model for the dynamic communication delay. The main idea is to utilize the existing wide-area protection system and guarantee the performance of regional and backbone networks, respectively.

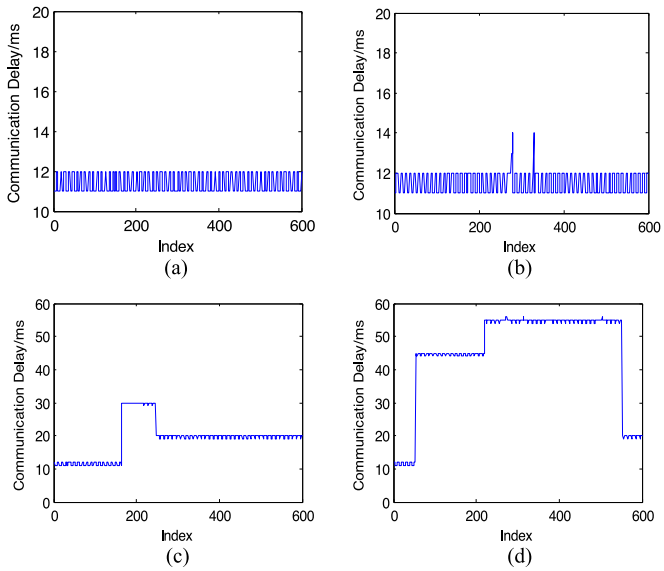

Fig. 2. Records of FNET communication delays in short-term (one minute).

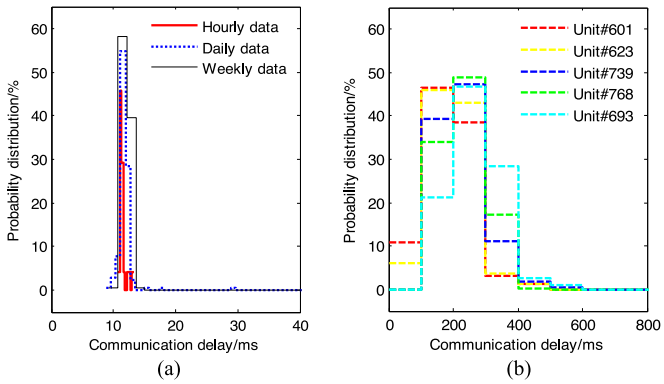

Fig. 3. Records of FNET communication delays in long-term (a few hours to a few days): (a) Statistical results of different time spans, and (b) Statistical results of different locations.

First, PDCs are utilized to limit the communication delay of complex regional networks. The communication delay between PMUs and PDCs primarily stems from the difference between the propagation time of synchrophasor data and the processing time of PDCs. Accordingly, the amount of $t_{RN} + t_{PDC}$ depends on the physical distance between PMUs/PDCs and PDCs (the communication path of a regional network is PMU, $\mathrm{PDC}_1, ..., \mathrm{PDC}_{NPDC}$), and the data arriving and sending-out time in PDCs.

IEEE Std C37.244 defines seventeen PDC functions as shown in Fig. 4. In reality, multiple PMU packages with the same time-tag may not arrive at a PDC simultaneously. The PDC assigns the early arriving data to a buffer (data buffering) and aligns the available data after the preset wait time (data aggregation). The "PDC wait time" or "relative wait time" in C37.244-2013 ensures that PDCs sort and forward PMU packages within an acceptable time period instead of waiting for delayed or lost packages blindly losing packages. Meanwhile, the PDC can

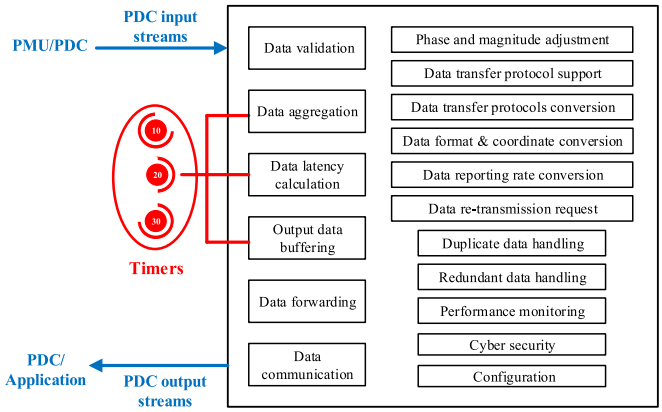

Fig. 4. Block diagram of PDC functions.

calculate the delay between a PMU and a PDC or between a PDC and another PDC using time-tags (data latency calculation). Hence, this work combines data aggregation, data latency calculation, and data buffering functions as shown in Fig. 4, and views the complex regional network as a black box. Then, in PDCs, the communication delay can be calculated with time-tags and further bounded through the wait time as

$$t_{RN}+t_{PDC}= \left[\sum_{k=1}^{N_{PDC}}\left(t_{cal\_k}+t_{proc\_k}\right),\ \sum_{k=1}^{N_{PDC}}\left(t_{cal\_k}+t_{wait\_k}+t_{proc\_k}\right)\right] \doteq \left[\sum_{k=1}^{N_{PDC}} t_{cal\_k},\quad D_{RN}/v+\sum_{k=1}^{N_{PDC}} t_{wait\_k}\right] \tag{2}$$

where N_{PDC} is the number of PDCs, t_{cal_k} is the calculated delay between PMU and PDC_1 or between PDC_k and PDC_{k+1}, t_{wait_k} is the wait time of PDC_k, and t_{proc_k} is the additional processing time of PDC_k. D_{RN} is the physical distance of the communication path in reginal networks. Normally, t_{proc_k} is much smaller than the other terms in (2) and is ignored here. The lower bound in (2) means that the PMU packages experience no wait time at each PDC (arriving at each PDC simultaneously), and the upper bound means that the PMU packages experience the whole preset wait time at every PDC.

Second, the communication delay over backbone networks is bounded owing to SONET/SDH implementation. Currently, SONET/SDH is globally deployed. In the U.S., thousands of miles of optical fibers have been installed as parts of power line facilities and SONET-based backbone networks have been employed by many utilities [39], [40]. In China, a large number of power industry backbone networks select optical fibers and SDH as the communication medium and protocol [41], [42]. SONET/SDH not only greatly improves the performance of power system communications, but also provides fast, reliable, and robust communication infrastructure for wide-area protection [9], [10], [39]–[42]. Here, the self-healing potential of SONET is utilized to guarantee the QoS of backbone networks and to further determine the bound of communication delays.

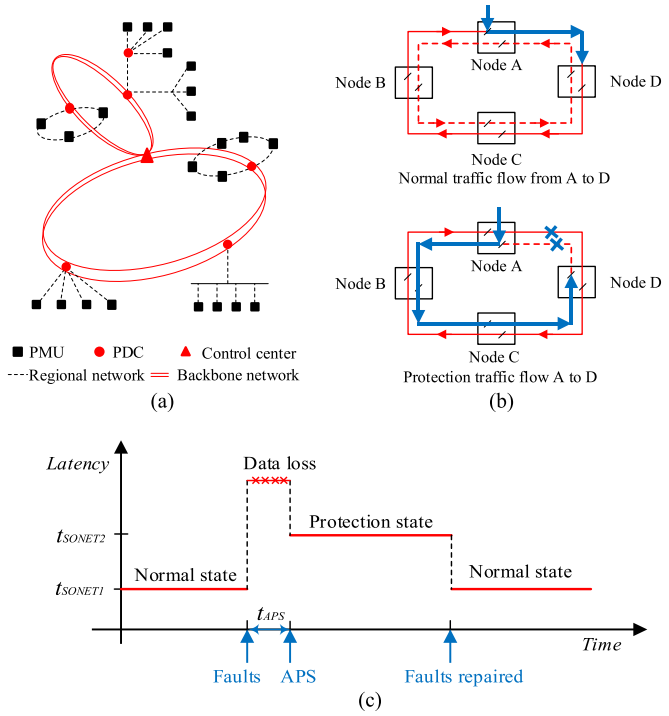

Fig. 5. Operating principle of SONT: (a) Hierarchical structure, (b) Automatic switching, and (c) Operating latency of automatic switching.

Typically, SONET works at the unidirectional path-switched ring or bidirectional line-switched ring (BLSR) mode. SONET realizes the self-healing and redundant communication using its ring topology and automatic protection switching (APS) scheme. In the normal state, the information is transmitted on the primary ring and a copy of the information travels via the protection ring; while in the case of a node or link failure, SONET automatically and quickly switches the information flow from the primary ring to the protection ring and sends out alarm signals. Also, SONET will resume the information flow to the original route when the equipment or fibers are repaired.

In terms of multiple failures, a four-fiber BLSR design can be used to increase SONET's fault tolerance capacities. Hence, SONET can improve the reliability of communication networks and guarantee the QoS of information transmission. The communication delay of SONET based backbone networks becomes predictable as shown in Fig. 5, and its bound can be calculated by (3) [32].

$$t_{BN}=\left[t_{SONET_1},\ t_{SONET_2}\right]+D_{BN}/v \tag{3}$$

where t_{SONET1} and t_{SONET2} are the SONET delays in the normal state and the protection state, respectively. D_{BN} is the physical distance of the communication path in backbone networks.

Note that the models in (2) and (3) assume SONET among backbone nodes and do not consider the communication system buffering or error correction (e.g., the ones in TCP/IP) [40]. Hence, assuming the communication path of wide-are protection as PMU/RegionalPDC/CentralPDC/SONET, the upper bound

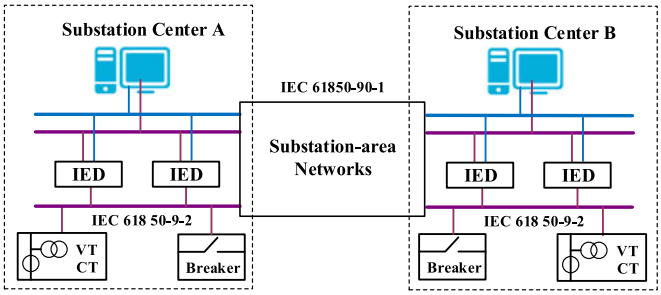

Fig. 6. Block diagram of a typical substation-area protection system.

of the communication delay can be determined as

$$t_d \leq \frac{D_{RN}}{v} + (t_{wait\_1} + t_{wait\_2}) + \frac{D_{BN}}{v} + t_{SONET_2} \quad (4)$$

III. Communication Delays of Substation-Area Protection

A. Substation-Area Protection

Substation-area protection involves the protection based on local measurements and dedicated to specific equipment, e.g., generator, transformer, and transmission line; it also covers the protection using the measurements between substations, such as directional comparison protection [43], [44]. Hence, substation-area protection needs the communications within a substation and between substations.

The International Electrotechnical Commission (IEC) releases the IEC 61850 standard to standardize the substation communication system. The IEC 61850 standard has been globally employed in recent years and, thus, is used here. According to IEC 61850, the communication network over substation areas is illustrated in Fig. 6. In one substation, the current and voltage values of instrument transformers and the state/condition information of breakers are digitally transmitted to the Ethernet bus and further routed to the intelligent electronic device (IED) integrating protection and control (P&C) functionalities. While between substations, the trip/close commands and the service information are interchanged through tunneling in order to implement certain protection functionalities. Also, according to IEC 61850, substation messages with different properties are classified into seven types: fast, medium-speed, low-speed, raw-data, file-transfer functions, time synchronization, and command with access control messages, respectively. As shown in Table I, the current and voltage values of instrument transformers, the states and trip/close commands of breakers, and the monitoring/maintenance/service information are modeled as sampled value (SV), generic object-oriented substation event (GOOSE), and manufacturing message standard (MMS), respectively [43]–[46].

Specifically, IEC 61850-5 defines the transfer time as the sum of the processing time at the sender and receiver and the transmission time (communication delay) over networks, and requires the transfer time of SV and GOOSE to be below 3 ms.

TABLE I
SV, GOOSE, and MMS Models in IEC 61850

Model	SV	GOOSE	MMS
Communication mechanism	Publisher/ subscriber	Publisher/ subscriber	Client/server
Message type	Raw-data msg.	Fast msg.	Others
Output type	Periodic	Burst	Burst
Sampling frequency	4000/12800 sps	10 sps	Depends
Packet length	169∼226 Byte	230 Byte	Depends
Propriety	High	Highest	Medium
Transmission time	3-10 ms	3-10 ms	Non time-critical

P.S. The package lengths of SV and GOOSE are flexible and their typical values are listed above. Also, the power system frequency is selected as 50 Hz here and sps means samples per second.

Fast and reliable communication networks play a fundamental role in substation-area protection. In practice, a large number of substations select Ethernet switches and optical fibers to establish switched Ethernet networks and successfully achieve the real-time communication and information sharing over substation areas. Substation-area protection is time-critical, and its communication delay is analyzed next.

B. Quantization of Communication Delays

To quantify the communication delay in a switched Ethernet network, two general approaches are used in the literature: stochastic approaches and deterministic approaches [47], [48]. The former studies the average behavior of a stochastic network and works out the mean statistical or probabilistic delay. For instance, the queuing theory assumes the distribution of delays as Poisson or Bernoulli and computes the mean value of delays and, possibly, the quantity of distributions. Regardless, time delays may not always follow a regular distribution in reality, and the upper bound of delays may not exist or may not be computable. In contrast, the latter focuses on the worst-case performance analysis and determines the upper bound of delays, which is mainly implemented using network calculus.

In substation-area protection, a protective relay is expected to effectively detect the fault and trip off the corresponding circuit breaker after a preprogrammed time delay. Meanwhile, SV and GOOSE packages should be transferred to IEDs within the predetermined time; otherwise, they are viewed as corrupted and lost, which may disable the protection functionality and endanger the substation or even the whole power grid. In practice, the time delay of protective relays needs to be set to a reasonable level. If the time delay is larger than the transfer time limit (e.g., 3 ms), the protection may be invalid, whereas if the time delay is set to be idealistic, package losses may frequently occur. The network calculus theory focuses on performance guarantees, instead of the classical queuing theory that deals with average values. Therefore, network calculus is used to model the communication delay here.

Network calculus, as a queueing theory for performance guarantee analysis of computer networks [47], was first introduced by Cruz for modeling network entities and flows [49]. In the past two decades, it has been generalized with alternate algebras such

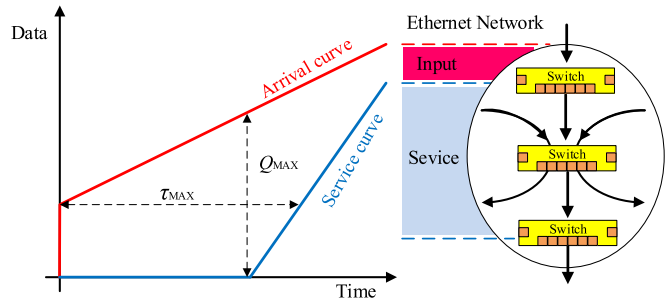

Fig. 7. Typical arrival and service curves, in which the delay bound $\tau_{\max}$ and backlog bound $Q_{\max}$ are given by the maximum horizontal and vertical distances between $\alpha(t)$ and $\beta(t)$, respectively.

as min-plus and max-plus algebra to transform complex network systems into analytically tractable systems [48]–[53]. Specifically, it introduces the concepts of arrival and service curves to model the traffic arrival process and the service process of a system, based on which network performance bounds are further analyzed. As shown in Fig. 7, an arrival curve $\alpha(t)$ in (5) upper-bounds the amount of traffic input of a data flow to a network system, and a service curve $\beta(t)$ in (6) lower-bounds the amount of service provided by the system to the data flow. These two curves collaboratively determine the delay bound $\tau_{\max}$ in (7) and backlog bound $Q_{\max}$ in (8).

$$\alpha(t) = rt + b \tag{5}$$

$$\beta(t) = R[t-\theta]^+ \tag{6}$$

$$\tau(t) \le \sup_{t\ge 0}\{inf\{\tau_{\max} : \alpha(t) \le \beta(t+\tau_{\max})\}\} \tag{7}$$

$$Q(t) \le Q_{\max} = \sup_{t\ge 0}\{\alpha(t) - \beta(t)\} \tag{8}$$

where (5) and (6) are constraints on the arrival and service processes of a data flow, which have an average traffic rate r with maximum instantaneous burst b and minimum service rate R with latency parameter θ, respectively. With the assumption of $r \le R$, it can be easily obtained that $\tau_{\max} = b/R + \theta$ and $Q_{\max} = b + r\theta$.

Recently, the network calculus theory has been applied to calculate the delay bound of intra-substation communications in [26], [27]. In addition, the idea of worst-case analysis as in network calculus was adopted in [28]. In the present work, network calculus is employed for delay bound analysis of substation-area communications where priority queuing is used to schedule different types of messages in the network. For this analysis, a summary of the related network calculus results is presented as follows.

For ease of expression, only one flow is used in the following to represent the traffic on the same end-to-end path. Denote the arrival and service curves for the data flow on path p with priority level i at server j as $\alpha^i_{j,p}$ and $\beta^i_{j,p}$. Accordingly, denote the arrival and service curves for the aggregate data flow on all paths with priority level i at server j as α^i_j and β^i_j. Let P_j represent the set of paths through server j. As to be discussed, in the network, all arrival curves and service curves can be represented using the types of (5) and (6).

Specifically, the following results are readily obtained from the network calculus theory [48], [50].

1) (P1) Superposition property
$$\alpha^i_j(t) = r^i_j t + b^i_j$$
with $r^i_j = \sum_{p\in p_j} r^i_{j,p}$ and $b^i_j = \sum_{p\in p_j} b^i_{j,p}$
2) (P2) "Leftover" service property under priority scheduling
$$\beta^i_j(t) = R^i_j\left[t-\theta^i_j\right]^+$$
with $R^i_j = C - r^1_j - \cdots - r^{i-1}_j$ and $\theta^i_j = \theta_j + (b^1_j + \cdots + b^{i-1}_j)/R^i_j$
3) (P2') Leftover service property under FIFO scheduling
$$\beta^i_{j,p}(t) = R^i_{j,p}\left[t-\theta^i_{j,p}\right]^+$$
with $R^i_{j,p} = R^i_j - r^i_j + r^i_{j,p}$ and $\theta^i_{j,p} = \theta^i_j + (b^i_j - b^i_{j,p})/R^i_{j,p}$
4) (P3) Output property
$$\alpha^{*i}_j(t) = r^i_j t + \left(b^i_j + r^i_j\theta^i_j\right)$$
$$\alpha^{*i}_{j,p}(t) = r^i_{j,p} t + \left(b^i_{j,p} + r^i_{j,p}\theta^i_{j,p}\right)$$
5) (P4) Concatenation property
$$\beta^i_p(t) = \beta^i_{1,p}(t) \otimes \cdots \otimes \beta^i_{n,p}(t)$$

Taking into account these properties and the delay and backlog service guarantee analysis property (P5), delay bounds for a feedforward network can be derived under a rather general and intuitive stability condition $r^i_j \le R^i_j$ [48]. In fact, under a stricter condition on the throughput, delay bound analysis can be extended to arbitrary network topology [50], [51].

For the system considered in this paper, the arrival and service curves of GOOSE and SV messages tagged with the highest and high priorities, at the first hop, can be written as

$$\begin{cases} \alpha^{GS}_{1,p}(t) = r^{GS}_{1,p} t + b^{GS}_{1,j} = \left(L^{GS}\times f^{GS}\right)t + L^{GS} \\ \alpha^{SV}_{1,p}(t) = r^{SV}_{1,p} t + b^{SV}_{1,j} = \left(L^{SV}\times f^{SV}\right)t + L^{SV} \end{cases} \tag{9}$$

$$\begin{cases} \beta^{GS}_1(t) = R^{GS}_1\left[t-\theta^{GS}_1\right]^+ = C\left[t-\frac{L^{GS}}{C}\right]^+ \\ \beta^{SV}_1(t) = R^{SV}_1\left[t-\theta^{SV}_1\right]^+ = \left(C-r^{GS}_1\right)\left[t-\frac{L^{GS}+b^{GS}_1}{C-r^{GS}_1}\right]^+ \end{cases} \tag{10}$$

where L^{GS} and L^{SV} are the maximum message lengths of GOOSE and SV messages, respectively, f^{GS} and f^{SV} are the frequencies of generating GOOSE and SV messages, respectively, and C is the switch port rate.

In this paper, L^{GS}, L^{SV}, f^{Gs}, f^{SV} and C are selected as 226 bytes, 230 bytes, 10 sps, 4000 sps, and 1000 Mbps, respectively [46]. A detailed explanation on the delay bound calculation using network calculus is presented in the Appendix.

IV. Case Study

In engineering, each protection application has specific requirements on the communication delay. For instance, the delay

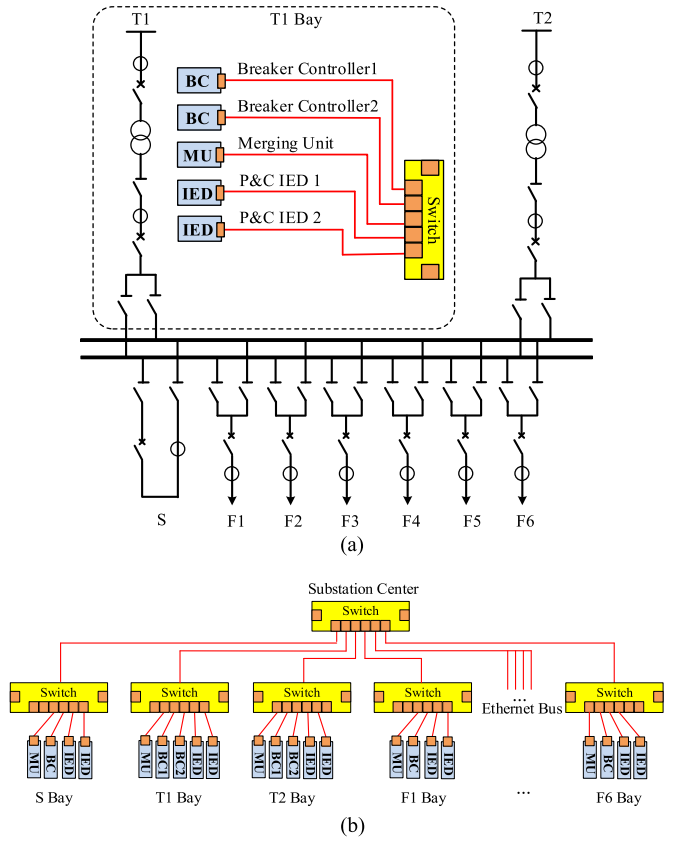

Fig. 8. IEC 61850 T2-2substation system: (a) Component connection diagram, and (b) Network connection diagram.

is required below 10 ms for primary protection, and is required to be from tens of milliseconds to a few seconds for backup protection in [41]. To further discuss the proposed bounded model for protection applications, the test studies of substation-area protection and wide-area protection are performed in this section.

A. *Case Study of Substation-Area Protection*

In terms of substation-area protection, the proposed bounded model is applied in the IEC 61850 T2-2 substation system as shown in Fig. 8 [19], [20]. The upper bounded communication delay in the T2-2 substation is calculated at 0.120 ms using the deterministic network calculus method. Meanwhile, the simulation is carried out with OPNET modeler, which is widely used for substation-communication simulations [19], [20] and [25]–[28]. The parameters can be found in [19] and [20], and the corresponding simulation results are shown in Fig. 9.

In addition to the communication in a single substation, the communication between two substations is also performed. Two IEC 61850 T2-2 substation systems that are 100 km apart are used, and the communication follows the IEC 61850-90-1 standard. The upper bounded communication delay is calculated as 0.572 ms, and the simulation results are presented in Fig. 10.

Figs. 9 and 10 show that the communication delays vary under different traffic conditions (the data stream rate is set to 35% for light traffic and 75% for heavy traffic). The communication delays in reality may violate the fixed or average value of constant or stochastic models, while they are all below the deterministic upper bounds 0.120 ms and 0.572 ms.

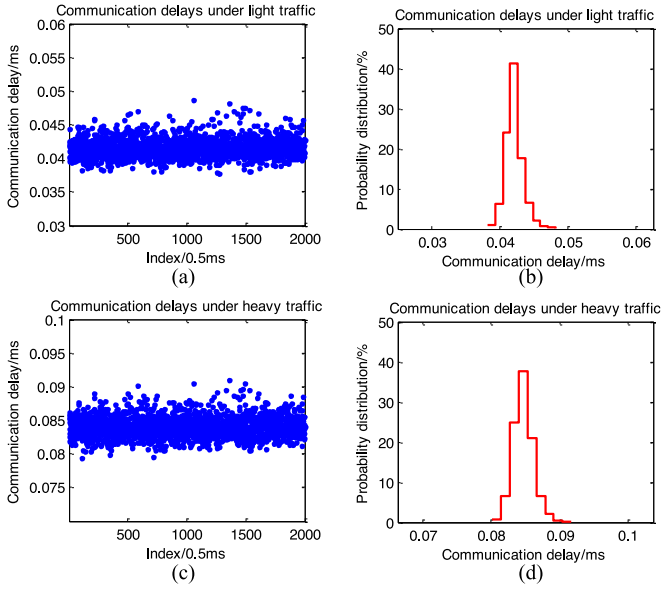

Fig. 9. SV delays in a substation.

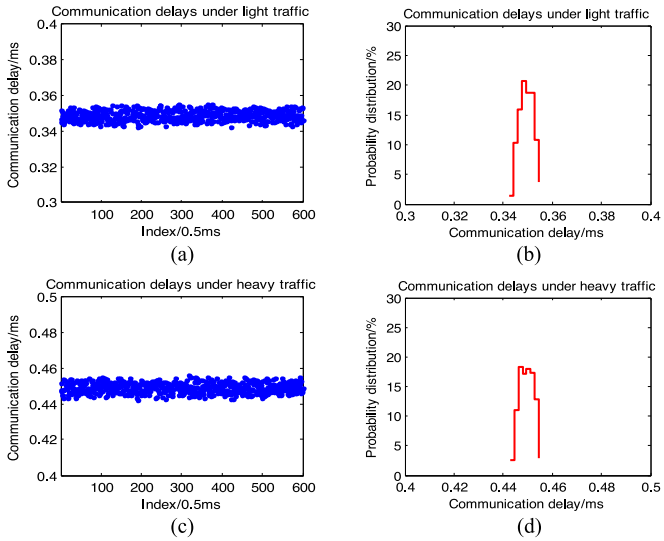

Fig. 10. GOOSE delays between two substations.

B. *Case Study of Wide-Area Protection*

In this case, the bounded model is employed in the IEEE 14 bus system as shown in Fig. 11. The parameters of the IEEE 14

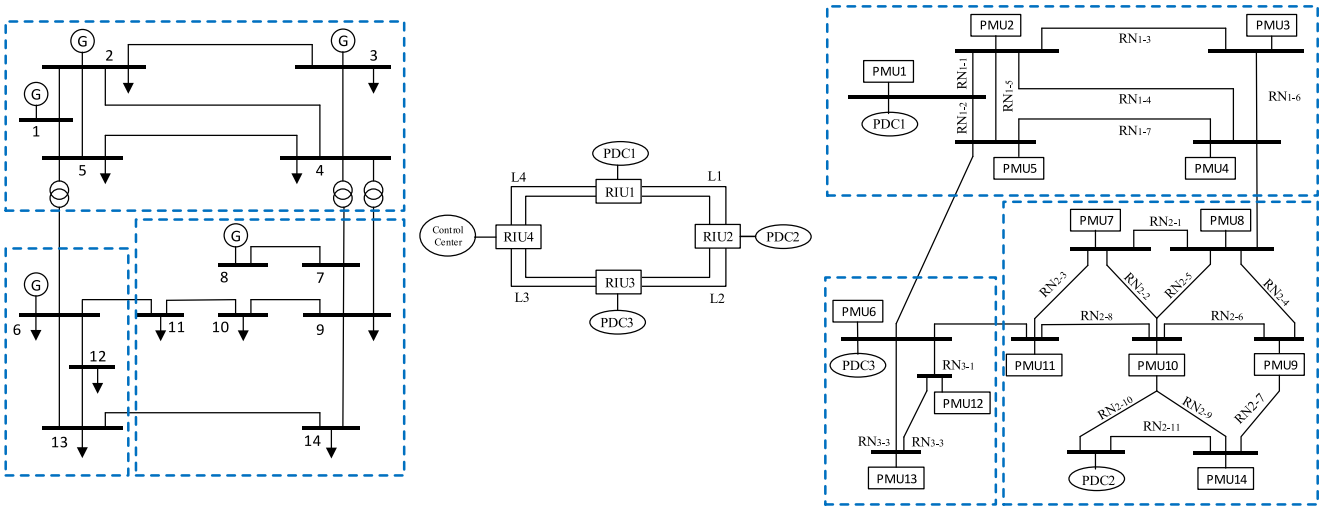

Fig. 11. IEEE 14 bus test system, which is dived into three areas according their geographical locations and voltage levels [15].

TABLE II
COMMUNICATION DELAYS BETWEEN PMUS AND PDCS

Conditions	Area	Max t_{prop} /ms	Min t_{prop} /ms	$t_{\mathrm{RN}} + t_{\mathrm{PDC}}$ /ms
Light traffic	Area 1	1.408	0.573	1.408
	Area 2	0.653	0.258	0.653
	Area 3	0.768	0.013	0.768
Heavy traffic	Area 1	1.408+	0.573	2.073
	Area 2	0.653+	0.258	1.058
	Area 3	0.768+	0.013	1.013

P.S. "+" denotes the additional propagation delay under heavy traffic.

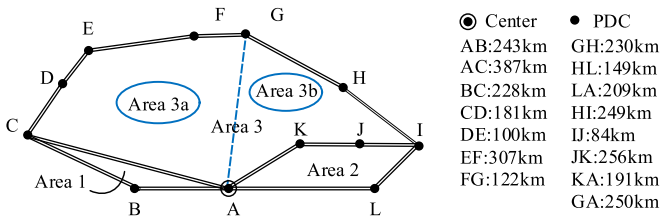

Fig. 12. SDH of China Southern Power Grid [42].

TABLE III
COMMUNICATION DELAYS BETWEEN PMUS AND APPLICATIONS

Conditions	Area	$t_{\mathrm{RN}} + t_{\mathrm{PDC}}$ /ms	t_{BN} /ms	t_{d} /ms
Light traffic	Area 1	1.408	1.459	2.867
	Area 2	0.653	1.056	1.709
	Area 3	0.788	0.603	1.391
Heavy traffic	Area 1	2.073	1.459	3.532
	Area 2	1.058	1.056	2.114
	Area 3	1.013	0.603	1.616
Heavy traffic + L1 break	Area 1	2.073	2.860	4.933
	Area 2	1.058	1.053	2.111
	Area 3	1.013	1.506	2.519
Heavy traffic + L2 break	Area 1	2.073	1.956	4.029
	Area 2	1.058	2.460	3.518
	Area 3	1.013	0.602	1.615
Heavy traffic + L3 break	Area 1	2.073	0.753	2.826
	Area 2	1.058	1.154	2.212
	Area 3	1.013	1.610	2.623

TABLE IV
COMMUNICATION DELAYS UNDER DIFFERENT NETWORK SCENARIOS

Conditions	Area	t_{d} /ms	Maximum t_{d} location
Original network	Area 1	[3.360, 4.078]	AB break
	Area 2	[4.413, 6.828]	IJ break
	Area 3	[9.269, 15.284]	FG break
Improved network	Area 3a	[5.566, 9.828]	DE break
	Area 3b	[5.706, 8.191]	IJ Break

bus system can be found in [15]. Here, the PMU package length is 2000 bits, the bandwidths of regional and backbone networks are 155 Mbps and 622 Mbps, respectively [18], and the preset wait times of PDC1, PDC2, and PDC3 are 1.50 ms, 0.80 ms, and 1.00 ms, respectively.

Assume that the regional network experiences the ideal and worst traffic, respectively, and that the backbone network suffers the L1, L2, and L3 break, respectively. As shown in Tables II and III, the communication delays under various traffics are bounded between 1.391 ms and 4.933 ms. The communication infrastructure in [15] and [18] provides a fast and reliable platform for wide-area protection.

Further, the bounded model is deployed in a larger system as shown in Fig. 12 [42]. For the sake of simplification, the communication delays between PMUs and PDCs as t_{RN} and are assumed to be 1 ms globally (the median value in Table II). The communication delays of three areas are listed in Table IV. It can be easily observed that t_d over wide backbone networks (Area 3) may be greater than the expected value 10 ms. To ensure the normal operation of protective devices, there are two possible solutions: increase the bandwidth of Network 3 or modify the topology of Area 3. Here, we adopt the latter due to its economy and add the link between AG. The results

are presented in Table IV as well. Hence, the advantages of the bounded model are two-fold: it not only provides latency bounds for relay setting but assists in the planning, design, and assessment of SIPS networks.

Admittedly, the relay setting, especially the delay setting, is not constrained by communications only. Some protective relays such as three-stage current relays and backup relays, shorten or prolong the time delay intentionally, according to the protection scheme design [8]–[10]. Therefore, in the SIPS design, communication constraints, SIPS operation requirements, and engineering experience need to be considered collectively.

V. Conclusion

The SIPS has received extensive attention in the last decade, especially with the rapid development of WAMS and IEC 61850 technologies. The SIPS extends the protection scope from local equipment to the integrity of a power system, and thus requires fast and reliable communications. This work focuses on the SIPS latency and proposes a new modeling method for the communication delay. The contributions of this research work can be summarized as follows.

First, the latency is investigated over wide areas and long terms, and a bounded model is proposed for the communication delay of wide-area protection. Since protection applications expect predictable or predetermined time delays for relay setting, the bounded model is more favorable than the constant or stochastic model in the literature. Specifically, the bounded model is derived from the existing infrastructure (e.g., PDC, SONET/SDH, and switched Ethernet network), which does not demand any not-yet-implemented hardware or technologies.

Second, the bounded model is applied for the communication delay of substation-area protection as well. Here, the network calculus theory is used, which deals with performance guarantees instead of average values in the classical queuing theory. Meanwhile, various factors such as the priorities of GOOSE and SV messages, the communications in a substation (IEC 61850-9-2), and the communications between substations (IEC 61850-90-1) are considered. The bounded model suggests the network's worst-case performance, and thus can be viewed as an important tool for protection engineers.

Moreover, the proposed model is employed in the IEC 61850 T2-2 substation system, IEEE 14 bus system, and China Southern Power Grid SDH system. It can be seen that the proposed model not only provides latency bounds for relay setting, but also plays an advantageous role in the planning, design and assessment of SIPS networks.

Future works may include analysis of the substation network with redundant configurations (e.g., using parallel redundancy protocols) and application of the proposed bounded communication delay in real SIPSs.

Appendix

This Appendix presents how the two delay bounds discussed in Section IV–A are derived using the network calculus theory. To clearly explain the derivation in this limited space, some assumptions and simplifications are made as follows:

1) The switched Ethernet network in each substation adopts a spanning tree protocol to route traffic. This is a standard setup for Ethernet networks to avoid traffic looping in the network.

2) Without loss of generality, we assume that the resultant spanning tree for each substation network is the tree where the root switch 1 (RS1) is on the root, all S-bay, T1-bay, T2-bay, F1-bay, ..., F5-bay switches are children nodes of RS1, and MU/BC/IED elements are children nodes of their corresponding S-bay/T1-bay/T2-bay/F1-bay, ...,/F5-bay nodes.

3) The broadcast feature of Ethernet is adopted for an MU/BC/IED to send messages. This implies that every packet sent by an MU/BC/IED will be received by all other MU/BC/IEDs, as well as the gateway, in the network. As a result, the network operates in the worst case, in terms of traffic load.

4) In each switch, the messages of different types are served in the priority scheduling manner, whereas the messages of the same type are served in the FIFO manner. Also, the buffer size of each switch is large enough, ensuring no packet loss when the traffic is constrained (i.e., $r_j^i \le R_j^i$).

5) For simplicity in expression, we assume that every MU sends SV messages and every bay is configured with one IED.

6) The propagation delay within the substation is ignored.

A. Delay Bound for the Single Substation Case

In this case, the longest path for SV messages and the longest path for GOOSE messages are considered for the worst-case analysis, which are $\mathrm{MU} \to \mathrm{S} \to \mathrm{RS1} \to \mathrm{F6} \to \mathrm{IED}$, and $\mathrm{BC/IED} \to \mathrm{S} \to \mathrm{RS1} \to \mathrm{F6} \to \mathrm{IED}$, respectively. An illustration of these two paths can be found in Fig. I.

Step 1: Considering GOOSE has higher priority than SV, the potential effect of GOOSE on the service provided to SV at each link is identified first. This effect in the network calculus theory is dependent on the (worst-case) bustiness of GOOSE traffic, and captured by the arrival curves as follows

$$\alpha^{GS}_{S/T1/T2/F1/\ldots/F5}(t) = 2r^{GS}\cdot t + 2L^{GS} \tag{A1}$$

$$\alpha^{GS}_{BC\to F6}(t) = r^{GS}\cdot t + L^{GS} \tag{A2}$$

$$\alpha^{GS}_{S/T1/T2/F1/\ldots/F5\to RS}(t) = 2r^{GS}\cdot t + 2L^{GS} + 2r^{GS}\times\frac{L}{C} \tag{A3}$$

$$\alpha^{GS}_{RS}(t) = \alpha^{GS}_{S+\ldots+F5\to RS}(t) = 16r^{GS}\cdot t + \left(16L^{GS} + 16r^{GS}\times\frac{L}{C}\right) \tag{A4}$$

$$\alpha^{GS}_{RS\to F6}(t) = 16r^{GS}\cdot t + \left(16L^{GS} + 16r^{GS}\times\frac{L}{C} + 16r^{GS}\times\frac{L}{C}\right) \tag{A5}$$

$$\alpha^{GS}_{F6}(t) = \alpha^{GS}_{RS\to F6}(t) + \alpha^{GS}_{BC\to F6}(t) = 17r^{GS}\cdot t + \left(17L^{GS} + 32r^{GS}\times\frac{L}{C}\right) \tag{A6}$$

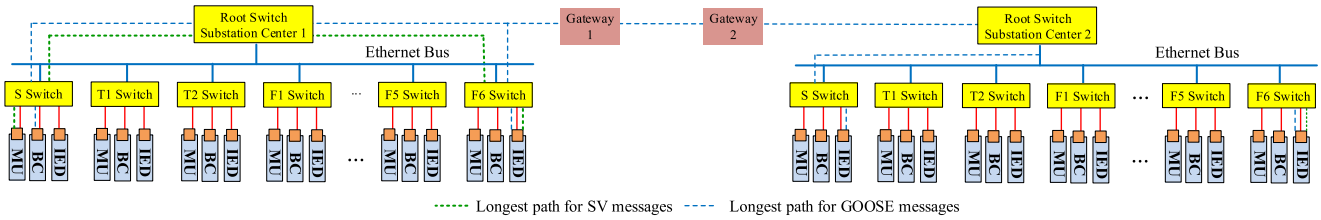

Fig. I. Diagram of network connection of two substations.

where α_n^{GS} denotes the arrival curve of GOOSE messages entering each node n on the path, and L denotes $\max(L^{\mathrm{GS}}, L^{\mathrm{SV}})$.

Step 2: With the effect of the GOOSE traffic above, the minimum amount of service that the SV traffic may receive at each node n is characterized using the service curve β_n^{SV} as

$$\beta_{S/T1/T2/F1/\ldots/F6/RS}\left(t\right) = C\left(t - \frac{L}{C}\right)^+ \tag{A7}$$

$$\beta^{SV}_{S/T1/T2/F1/\ldots/F5}\left(t\right) = \left(C - 2r^{GS}\right)\left(t - \frac{L + 2L^{GS}}{C - 2r^{GS}}\right)^+ \tag{A8}$$

$$\begin{aligned}\beta^{SV}_{RS}\left(t\right) &= \beta_{RS}\left(t\right) - \alpha^{GS}_{RS}\left(t\right)\\ &= \left(C - 16r^{GS}\right)\left(t - \frac{L + 16L^{GS} + 16L^{GS} \times \frac{L}{C}}{C - 16r^{GS}}\right)^+\end{aligned} \tag{A9}$$

$$\begin{aligned}\beta^{SV}_{F6}\left(t\right) &= \beta_{F6}\left(t\right) - \alpha^{GS}_{F6}\left(t\right)\\ &= \left(C - 17r^{GS}\right)\left(t - \frac{L + 17L^{GS} + 32L^{GS} \times \frac{L}{C}}{C - 17r^{GS}}\right)^+\end{aligned} \tag{A10}$$

Step 3: Accordingly, the arrival curves of SV messages α_n^{SV} at each node n, can be written in (A11) to (A13).

$$\alpha^{SV}_{S/T1/T2/F1/\ldots/F6}\left(t\right) = r^{SV} \cdot t + L^{SV} \tag{A11}$$

$$\alpha^{SV}_{T1/T2/F1/\ldots/F5\rightarrow RS}\left(t\right) = r^{SV} \cdot t + L^{SV} + L + 2L^{GS} \tag{A12}$$

$$\alpha^{SV}_{T1+T2+F1+\ldots+F5\rightarrow RS}\left(t\right) = 7r^{SV} \cdot t + 7L^{SV} + 7L + 14L^{GS} \tag{A13}$$

Step 4: In this step, an end-to-end service curve for the SV traffic crossing the whole end-to-end path is obtained. The idea here is to consider the effect of FIFO scheduling resulting from the SV traffic that later joins and shares the longest path. There are two sub-steps.

First, let's view $\mathrm{RT} + \mathrm{F6}$ as a virtual server to all SV traffic sharing $\mathrm{RS1} \rightarrow \mathrm{F6} \rightarrow \mathrm{IED}$, where the FIFO effect for the SV traffic generated by MU connected to F6 is taken out. At the second sub-step, we first take out the FIFO effect from the SV traffic generated by MUs connected to $\mathrm{T1}, \mathrm{T2}, \mathrm{F1}, \ldots$, and F5, at the virtual server $\mathrm{RS1} + \mathrm{F6}$, and we denote the obtained service curve as

$$\begin{aligned}\beta^{SV}_{RS\rightarrow F6}\left(t\right) &= \left(\mathrm{C} - 17r^{GS} - r^{SV}\right)\\ &\times \left(t - \frac{L + 17L^{GS} + 32r^{GS} \times \frac{L}{C}}{C - 17r^{GS} - r^{SV}} - \frac{L^{SV}}{C - 17r^{GS}}\right)^+\end{aligned} \tag{A14}$$

$$\begin{aligned}\beta^{SV}_{RS} \otimes \beta^{SV}_{RS\rightarrow F6}\left(t\right) &= \left(\mathrm{C} - 17r^{GS} - r^{SV}\right)\\ &\times \left(t - \frac{2L + 33L^{GS} + 48r^{GS} \times \frac{L}{C}}{C - 17r^{GS} - r^{SV}} - \frac{L^{SV}}{C - 17r^{GS}}\right)^+\end{aligned} \tag{A15}$$

Then, we integrate it with the S-bay switch on the path, and use the network calculus concatenation property to obtain the end-to-end service curve for the SV traffic crossing the whole path.

$$\begin{aligned}\beta^{SV-Path}_{RS+F6}\left(t\right) &= \left(\mathrm{C} - 17r^{GS} - 8r^{SV}\right)\\ &\times \left(t - \frac{2L + 33L^{GS} + 48r^{GS} \times \frac{L}{C}}{C - 17r^{GS} - 8r^{SV}} - T_2 - T_3\right)^+\end{aligned} \tag{A16}$$

$$\begin{aligned}\beta^{SV}_{Path}\left(t\right) &= \beta^{SV}_{S} \otimes \beta^{SV-Path}_{RS+F6}\left(t\right)\\ &= \left(\mathrm{C} - 17r^{GS} - 8r^{SV}\right)\left(t - T_1 - T_2 - T_3\right)^+\end{aligned} \tag{A17}$$

with $T_1 = \frac{3L + 35L^{GS} + 48r^{GS} \times \frac{L}{C}}{C - 17r^{GS} - 8r^{SV}}$, $T_2 = \frac{7L^{SV} + 7L + 14L^{GS}}{C - 17r^{GS} - r^{SV}}$, and $T_3 = \frac{L^{SV}}{C - 17r^{GS}}$.

Step 5: In the final step, the delay bound for the SV traffic is easily obtained as

$$t_d^{SV} \leq \frac{L^{SV}}{C - 17r^{GS} - 8r^{SV}} + T_1 + T_2 + T_3 \tag{A18}$$

In these steps, the various network calculus results as summarized in Section III.B have been applied. Specifically, Step 1 and Step 3 are mainly based on the superposition property and the output property, Step 2 makes use of the left-over service property under priority scheduling, Step 4 relies on the service curve property under FIFO scheduling together with the concatenation property, and Step 5 is a direct application of the service guarantee analysis property.

B. Delay Bound for the Two Substation Case

In this case, GOOSE messages are transmitted between two substations. The resultant longest path becomes: $\mathrm{BC} \rightarrow \mathrm{S} \rightarrow \mathrm{RS1} \rightarrow \mathrm{Gateway1}\ \ (\mathrm{GT1}) \rightarrow \mathrm{Gateway2}\ \ (\mathrm{GT2}) \rightarrow \mathrm{RS2} \rightarrow \mathrm{S} \rightarrow \mathrm{IED}$. The analysis follows the similar steps.

Step 1: On the end-to-end path, there are two GOOSE message flows, generated by BCs and IEDs, which share the S-bay switch in the FIFO manner in Substation 1 network. Due to FIFO, both flows have the same end-to-end delay bound, and they can be treated together as one flow, whose arrival curve is

$$\alpha_S^{GS}(t) = 2r^{GS} \cdot t + 2L^{GS} \tag{A19}$$

Step 2: At the RS1, RS2, and S-bay switch in the Substation 2, there are other GOOSE message flows sharing the respective rest of the longest path in the FIFIO manner. Their arrival curves can be written as

$$\alpha^{GS}_{T1+T2+F1+\cdots+F6\rightarrow RS1}(t) = 16r^{GS} \cdot t + 16L^{GS} + 16r^{GS} \times \frac{L}{C} \tag{A20}$$

$$\alpha^{GS}_{T1+T2+F1+\cdots+F6\rightarrow RS2}(t) = 16r^{GS} \cdot t + 16L^{GS} + 16r^{GS} \times \frac{L}{C} \tag{A21}$$

$$\alpha^{GS}_{BC\rightarrow S}(t) = r^{GS} \cdot t + L^{GS} \tag{A22}$$

Step 3: In this step, an end-to-end service curve for the GOOSE traffic crossing the whole end-to-end path is obtained. Since GOOSE has the highest priority, the service curve for all GOOSE traffic at every node on the path is as follows

$$\beta^{GS}_{S/RS1/GT1/GT2/RS2/S}(t) = C\left(t - \frac{L}{C}\right)^+ \tag{A23}$$

The next step is to consider the effect of FIFO scheduling resulting from the GOOSE traffic that later joins and shares the longest path. Let's first consider the S switch for the GOOSE traffic on $\mathrm{BC} \rightarrow \mathrm{S} \rightarrow \mathrm{RS1} \rightarrow \mathrm{GT1} \rightarrow \mathrm{GT2} \rightarrow \mathrm{RS2} \rightarrow \mathrm{S}$, which provides the following service curve.

$$\beta^{GS}_{\rightarrow S}(t) = \left(C - r^{GS}\right)\left(t - \frac{L}{C - r^{GS}} - \frac{L^{GS}}{C}\right)^+ \tag{A24}$$

Consider $\mathrm{RS2} + \mathrm{S}$ together for all GOOSE traffic that passes them on the path, whose service curve, from the concatenation property, is given by

$$\beta^{GS}_{RS2+S}(t) = \left(C - r^{GS}\right)\left(t - \frac{2L}{C - r^{GS}} - \frac{L^{GS}}{C}\right)^+ \tag{A25}$$

Then, for the GOOSE traffic on $\mathrm{BC} \rightarrow \mathrm{S} \rightarrow \mathrm{RS1} \rightarrow \mathrm{GT1} \rightarrow \mathrm{GT2} \rightarrow \mathrm{RS2} \rightarrow \mathrm{S}$, the service curve below is provided to it by $\mathrm{RS2} + \mathrm{S}$.

$$\beta^{GS}_{\rightarrow RS2+S}(t) = \left(C - 17r^{GS}\right)\left(t - \frac{b_1}{C - 17r^{GS}} - \frac{b_2}{C - r^{GS}}\right)^+ \tag{A26}$$

where $b_1 = 2L + \left(C - r^{GS}\right)\frac{L^{GS}}{C}$ and $b_2 = 16L^{GS} + 16r^{GS} \times \frac{L}{C}$.

Third, since the GOOSE traffic through RS1, GT1 and GT2 is the same on $\mathrm{BC} \rightarrow \mathrm{S} \rightarrow \mathrm{RS1} \rightarrow \mathrm{GT1} \rightarrow \mathrm{GT2} \rightarrow \mathrm{RS2}$, the service curve for it by the path is easily found based on the concatenation property as

$$\begin{aligned}\beta^{GS}_{RS1+\cdots+S}(t) &= \beta^{GS}_{RS1} \otimes \beta^{GS}_{GT1} \otimes \beta^{GS}_{GT2} \otimes \beta^{GS}_{\rightarrow RS2}(t) \\ &= \left(\mathrm{C} - 17r^{GS}\right)\left(t - \frac{3L + b_1 + b_2}{C - 17r^{GS}}\right)^+\end{aligned} \tag{A27}$$

Fourth, at RS1, there is other GOOSE traffic, i.e., from $\mathrm{T1/T2/F1/}\cdots\mathrm{/F6}$, joining and sharing the path from RS1 using FIFO. With the consideration of this, the service provided to the GOOSE traffic that is already on the path has a service curve as

$$\begin{aligned}\beta^{GS}_{\rightarrow RS1+\cdots+S}(t) &= \left(\mathrm{C} - 33r^{GS}\right) \\ &\quad \times \left(t - \frac{3L + b_1 + \frac{C - 17r^{GS}}{C - r^{GS}} b_2}{C - 33r^{GS}} - \frac{b_2}{C - 17r^{GS}}\right)^+\end{aligned} \tag{A28}$$

Following the similar approach, concatenating S with $\rightarrow \mathrm{RS1} + \cdots + \mathrm{S}$, the end-to-end path provides the GOOSE traffic from BC and IED at the S-bay switch a service curve as follows

$$\begin{aligned}\beta^{GS}_{path}(t) &= \beta^{GS}_{S+RS1+\cdots+S}(t) = \beta^{GS}_{S} \otimes \beta^{GS}_{\rightarrow RS1+\cdots+S}(t)\,\beta \\ &= \left(\mathrm{C} - 33r^{GS}\right)\left(t - \frac{4L + b_1 + \frac{C - 17r^{GS}}{C - r^{GS}} b_2}{C - 33r^{GS}} - \frac{b_2}{C - 17r^{GS}}\right)^+\end{aligned} \tag{A29}$$

Step 4: In the final step, the following bound on delay for the GOOSE traffic is obtained as

$$t_d^{GS} \leq \frac{2L^{GS}}{C - 33r^{GS}} + T_1 + T_2 + T_3 \tag{A30}$$

where $T_1 = \frac{4L + b_1 + \frac{C - 17r^{GS}}{C - r^{GS}} b_2}{C - 33r^{GS}}$, $T_2 = \frac{b_2}{C - 17r^{GS}}$, and T_3 is the propagation delay between GT1 and GT2.

Remark: The delay bound analysis in this Appendix has chosen a simple way of applying the five basic properties of network calculus, for ease of expression. We remark that improved delay bounds may be obtained by exploiting these properties in a more advanced way, e.g., as in [53].

ACKNOWLEDGMENT

The authors would like to thank Dr. R Sun at Dominion Virginia Power and H. Zhang at NR (NARI Relay) Electric Co. Ltd. for providing technical support. The authors would also like to thank the editors and reviewers for their insightful comments and suggestions on improving the quality of this work.

REFERENCES

[1] A. Abdelmoumene and H. Bentarzi, "A review on protective relays' developments and trends," *J. Energy Southern Africa*, vol. 25, no. 2, pp. 91–95, May 2014.

[2] B. A. Oza and S. M. Brahma, "Development of power system protection laboratory through senior design projects," *IEEE Trans. Power Syst.*, vol. 20, no. 2, pp. 532–537, May 2005.

[3] T. S. Sidhu, M. S. Sachdev, and R. Das, "Modern relays: Research and teaching using PCs," *IEEE Comput. Appl. Power*, vol. 10, no. 2, pp. 50–57, Apr. 1997.

[4] U.S.-Canada Power System Outage Task Force, Final Report on the August 14, 2003 Blackout in the United States and Canada: Causes and Recommendations, Apr. 2004, Canada. [Online]. Available: https://reports.energy.gov/BlackoutFinal-Web.pdf.

[5] North American Electric Reliability Corporation (NERC), Events Analysis: System Disturbance Reports, 1996–2001, Washington, DC. [Online]. Available: http://www.nerc.com/pa/rrm/ea/System%20Disturbance%20Reports%20DL/Forms/AllItems.aspx

[6] P. Anderson and B. K. LeReverend, "Industry experience with special protection schemes," *IEEE Trans. Power Syst.*, vol. 11, no. 3, pp. 1166–1179, Aug. 1996.

[7] V. Madani *et al.*, "IEEE PSRC report on global industry experiences with system integrity protection schemes (SIPS)," *IEEE Trans. Power Del.*, vol. 25, no. 4, pp. 2143–2155, Oct. 2010.

[8] J. Xiao, F. Wen, C. Y. Chung, and K. P. Wong, "Wide-area protection and its applications—A bibliographical survey," in *Proc. IEEE PES PSCE*, 2006, pp. 1388–1397.

[9] M. G. Adamiak, A. P. Apostolov, M. M. Begovic, C. F. Henville, K. E. Martin, G. L. Michel, A. G. Phadke, and J. S. Thorp, "Wide area protection—Technology and infrastructures," *IEEE Trans. Power Del.*, vol. 21, no. 2, pp. 601–609, Apr. 2006.

[10] M. Begovic, D. Novosel, D. Karlsson, C. Henville, and G. Michel, "Wide area protection and emergency control," *Proc. IEEE*, vol. 93, no. 5, pp. 876–891, May 2005.

[11] K. Tomsovic, D. Bakken, V. Venkatasubramanian, and A. Bose, "Designing the next generation of real-time control, communication, and computations for large power systems," *Proc. IEEE*, vol. 93, no. 5, pp. 965–979, May 2005.

[12] V. Terzija *et al.*, "Wide-area monitoring, protection, and control of future electric power networks," *Proc. IEEE*, vol. 99, no. 1, pp. 80–93, Jan. 2011.

[13] P. Gao, M. Wang, S. G. Ghiocel, J. H. Chow, B. Fardanesh, and G. Stefopoulos, "Missing data recovery by exploiting low-dimensionality in power system synchrophasor measurements," *IEEE Trans. Power Syst.*, vol. 31, no. 2, pp. 1006–1013, Mar. 2016.

[14] Y. Zhu, J. Yan, Y. Tang, Y. L. Sun, and H. He, "Resilience analysis of power grids under the sequential attack," *IEEE Trans. Inf. Forens. Security*, vol. 9, no. 12, pp. 2340–2354, Dec. 2014.

[15] Y. Wang, W. Li, and J. Lu, "Reliability analysis of wide-area measurement system," *IEEE Trans. Power Del.*, vol. 25, no. 3, pp. 1483–1491, Jul. 2010.

[16] K. Zhu and L. Nordström, "Design of wide-area damping systems based on the capabilities of the supporting information communication technology infrastructure," *IET Gen., Transm. Distrib.*, vol. 8, no. 4, pp. 640–650, 2014.

[17] K. Zhu, M. Chenine, and L. Nordström, "ICT architecture impact on wide area monitoring and control systems' reliability," *IEEE Trans. Power Del.*, vol. 26, no. 4, pp. 2801–2808, Oct. 2011.

[18] P. Kansal and A. Bose, "Bandwidth and latency requirements for smart transmission grid applications," *IEEE Trans. Smart Grid*, vol. 3, no. 3, pp. 1344–1352, Sep. 2012.

[19] T. S. Sidhu and Y. Yin, "Modeling and simulation for performance evaluation of IEC 61850-substation communication systems," *IEEE Trans. Power Del.*, vol. 22, no. 3, pp. 1482–1489, Jul. 2007.

[20] M. S. Thomas and I. Ali, "Reliable, fast, and deterministic substation communication network architecture and its performance simulation," *IEEE Trans. Power Del.*, vol. 25, no. 4, pp. 2364–2370, Oct. 2010.

[21] F. Zhang, Y. Sun, L. Cheng, X. Li, J. H. Chow, and W. Zhao, "Measurement and modeling of delays in wide-area closed-loop control systems," *IEEE Trans. Power Syst.*, vol. 30, no. 5, pp. 2426–2433, Sep. 2015.

[22] M. G. Kanabar, T. S. Sidhu, and M. R. D. Zadeh, "Laboratory investigation of IEC61850-9-2-based busbar and distance relaying with corrective measure for sampled value loss/delay," *IEEE Trans. Power Del.*, vol. 26, no. 4, pp. 2587–2595, Oct. 2011.

[23] C. Lu, X. Zhang, X. Wang, and Y. Han, "Mathematical expectation modeling of wide-area controlled power systems with stochastic time delay," *IEEE Trans. Smart Grid*, vol. 6, no. 3, pp. 1511–1519, May 2015.

[24] J. W. Stahlhut, T. J. Browne, G. T. Heydt, and V. Vittal, "Latency viewed as a stochastic process and its impact on wide area power system control signals," *IEEE Trans. Power Syst.*, vol. 23, no. 1, pp. 84–91, Feb. 2008.

[25] D. M. E. Ingram, P. Schaub, R. R. Taylor, and D. A. Campbell, "Performance analysis of IEC 61850 sampled value process bus networks," *IEEE Trans. Ind. Inf.*, vol. 9, no. 3, pp. 1445–1454, Aug. 2013.

[26] H. Georg, N. Dorsch, M. Putzke, and C. Wietfeld, "Performance evaluation of time-critical communication networks for smart grids based on IEC 61850," in *Proc. IEEE INFOCOM*, 2013, pp. 143–148.

[27] N. Dorsch, H. Georg, and C. Wietfeld, "Analyzing the real-time capability of wide area communication in smart grids," in *Proc. IEEE INFOCOM*, 2014, pp. 682–687.

[28] C. Zhu, C. Huang, J. Zheng, and Y. Yue, "Real-time measurement of communication subsystem of intelligent electronic device," in *Proc. ICEICE*, 2011, pp. 626–629.

[29] N. T. Anh, L. Vanfretti, J. Driesen, and D. Van Hertem, "A quantitative method to determine ICT delay requirements for wide-area power system damping controllers," *IEEE Trans. Power Syst.*, vol. 30, no. 4, pp. 2023–2030, Jul. 2015.

[30] F. Bai *et al.*, "Design and implementation of a measurement-based adaptive wide-area damping controller considering time delays," *Elect. Power Syst. Res.*, vol. 130, pp. 1–9, Jan. 2016.

[31] K. C. Lee, S. Lee, and M. H. Lee, "Worst case communication delay of real-time industrial switched Ethernet with multiple levels," *IEEE Trans. Ind. Electron.*, vol. 53, no. 5, pp. 1669–1676, Oct. 2006.

[32] W. Liu, H. Luo, S. Li, and D. Gao, "Investigation and modeling of communication delays in wide area measurement system," in *Proc. Asia-Pacific Power Energy Eng. Conf.*, 2012, pp. 1–4.

[33] Y. Liu, L. Zhan, Y. Zhang, P. N. Markham, D. Zhou, J. Guo, Y. Lei, G. Kou, W. Yao, J. Chai, and Y. Liu, "Wide-area measurement system development at the distribution level: An FNET/GridEye example," *IEEE Trans. Power Del.*, vol. 31, no. 2, pp. 721–731, Apr. 2016.

[34] D. Zhou, J. Guo, Y. Zhang, J. Chai, H. Liu, Y. Liu, C. Huang, X. Gui, and Y. Liu, "Distributed data analytics platform for wide-area synchrophasor measurement systems," *IEEE Trans. Smart Grid*, vol. PP, no. 99, pp. 1–9, 2016.

[35] L. Zhan, Y. Liu, J. Culliss, J. Zhao, and Y. Liu, "Dynamic single-phase synchronized phase and frequency estimation at the distribution level," *IEEE Trans. Smart Grid*, vol. 6, no. 4, pp. 2013–2022, Jul. 2015.

[36] W. Ju, J. Qi, and K. Sun, "Simulation and analysis of cascading failures on an NPCC power system test bed," in *Proc. IEEE Power Energy Soc. Gen. Meeting*, 2015, pp. 1–5.

[37] T. Ding, K. Sun, C. Huang, Z. Bie, and F. Li, "Mixed-integer linear programming-based splitting strategies for power system islanding operation considering network connectivity," *IEEE Syst. J.*, vol. PP, no. 99, pp. 1–10, 2016.

[38] F. Hu, K. Sun, A. D. Rosso, E. Farantatos, and N. Bhatt, "Measurement-based real-time voltage stability monitoring for load areas," *IEEE Trans. Power Syst., vol. 31, no. 4, pp. 2787–2798*, Jul. 2016.

[39] North American SynchroPhasor Initiative (NASPI), NASPI 2014 Survey of Synchrophasor System Networks - Results and Findings, Jul. 2015, United States. [Online] Available: https://www.naspi.org/documents

[40] *IEEE Standard for Synchrophasor Data Transfer for Power Systems*, IEEE Standard C37.118.2-2011, 2011.

[41] *General Specification of Transmitting Protection Information on Optical Channel*, China Electricity Council, DL/T 364-2010, 2010.

[42] W. Zhang, "Calculation and analysis about transmission time delay of SDH self-healing loop network," *Telecommun. Elect. Power Syst.*, vol. 26, no. 154, pp. 56–60, Aug. 2005.

[43] J. Wu, D. Dostanov, and M. Redfern, "Fault passage protection based on IDMT relaying with IEC61850-90 inter-substation communications," in *Proc. 12th IET Int. Conf. Develop. Power System Protect.*, 2014, pp. 1–6.

[44] N.-K. C. Nair and D. L. P. Jenkins, "IEC 61850 enabled automatic bus transfer scheme for primary distribution substations," *IEEE Trans. Smart Grid*, vol. 4, no. 4, pp. 1821–1828, Dec. 2013.

[45] L. Zhu, D. Shi, and P. Wang, "IEC 61850-based information model and configuration description of communication network in substation automation," *IEEE Trans. Power Del.*, vol. 29, no. 1, pp. 97–107, Feb. 2014.

[46] C. Huang, C. Xiao, Y. Fang, and J. Zheng, "A method to deal with packet transfer delay of sampled value in smart substation," *Power System Technol.*, vol. 35, no. 1, pp. 5–10, 2011.

[47] Y. Jiang, "Network calculus and queueing theory: Two sides of one coin," in *Proc. 4th Int. Conf. Performance Eval. Method. Tools*, 2009, pp. 1–11.

[48] Y. Jiang and Y. Liu, *Stochastic Network Calculus*, New York, USA: Springer, 2008.

[49] R. L. Cruz, "A calculus for network delay, part I and part II," *IEEE Trans. Inf. Theory*, vol. 37, no. 1, pp. 114–141, Jan. 1991.

[50] J.-Y. Le Boudec and P. Thiran, *Network Calculus: A Theory of Detministic Queueing Systems for the Internet*, Berlin, Germany: Springer-Verlag, 2001.
[51] Y. Jiang, "Delay bounds for a network of guaranteed rate servers with FIFO aggregation," *Comput. Netw.*, vol. 40, no. 6, pp. 683–694, 2002.
[52] Y. Jiang, "A basic stochastic network calculus," in *Proc. ACM SIGCOMM Conf*, 2006, pp. 123–134.
[53] L. Lenzini, E. Mingozzi, and G. Stea, "A methodology for computing end-to-end delay bounds in FIFO-multiplexing tandems," *Perf. Eval.*, vol. 65, no. 11–12, pp. 922–943, 2008.

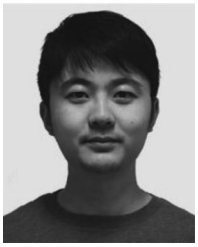

Can Huang (S'13) received the B.S.E.E degree from Hohai University, Nanjing, China, in 2008, the M.S.E.E. degree from Southeast University, Nanjing, China, in 2011. and is currently pursuing the Ph.D. degree in electrical engineering at the University of Tennessee, Knoxville, TN, USA.

From 2011 to 2012, he was with the State Grid Electric Power Research Institute (NARI Group Corporation), Nanjing. His current research interests include renewable energy, power system operation and control, and IT applications in power system measurement, protection, and communication.

Fangxing Li (S'98–M'01–SM'05) is also known as Fran Li. He received the B.S.E.E. and M.S.E.E. degrees from Southeast University, Nanjing, China, in 1994 and 1997, respectively, and the Ph.D. degree in electrical and computer engineering from Virginia Polytechnic Institute and State University, Blacksburg, VA, USA, in 2001.

From 2001 to 2005, he was with ABB Electric Systems Consulting (ESC), Raleigh, NC, USA. Currently, he is an Associate Professor in electrical engineering and the Campus Director of CURENT at the University of Tennessee, Knoxville, TN, USA. His current research interests include renewable energy integration, distributed generation, energy markets, power system computing and simulation, and phasor measurement unit-based voltage stability.

Prof. Li is presently is the Vice Chair of IEEE Power and Energy Society PSPI Committee, an Editor of the IEEE TRANSACTIONS ON SUSTAINABLE ENERGY, an Editor of IEEE Power and Energy Society Letters, a Guest Editor of the IEEE TRANSACTIONS ON SMART GRID, a Fellow of IET, and a registered Professional Engineer (P.E.) in the State of North Carolina.

Tao Ding (S'13–M'15) received the B.S.E.E. and M.S.E.E. degrees from Southeast University, Nanjing, China, in 2009 and 2012, respectively, and the Ph.D. degree in electrical engineering from Tsinghua University, Beijing, China, in 2015.

From 2013 to 2014, he was a Visiting Scholar with the Department of Electrical Engineering and Computer Science, the University of Tennessee, Knoxville, TN, USA. Currently, he is an Associate Professor in the State Key Laboratory of Electrical Insulation and Power Equipment, School of Electrical Engineering, Xi'an Jiaotong University, Xi'an, Shaanxi, China. His current research interests include electricity markets, power system economics and optimization methods, power system planning and reliability evaluation, and phasor-measurement-unit-based applications.

Yuming Jiang (SM'14) received the B.Sc. degree in electronic engineering from Peking University, Beijing, China, in 1988, the M.Eng. degree in computer science and engineering from Beijing Institute of Technology, Beijing, China, in 1991, and the Ph.D. degree in electrical and computer engineering from the National University of Singapore, Singapore, in 2001.

From 1996 to 1997, he was with Motorola, Beijing, China. From 2001 to 2003, he was a Member of Technical Staff and a Research Scientist with the Institute for Infocomm Research, Singapore. From 2003 to 2004, he was an Adjunct Assistant Professor with the Department of Electrical and Computer Engineering, National University of Singapore. From 2004 to 2005, he was with the Centre for Quantifiable Quality of Service in Communication Systems, Norwegian University of Science and Technology (NTNU), Trondheim, Norway. Since 2005, he has been a Professor with the Department of Telematics, NTNU. He is the first author of *Stochastic Network Calculus*. His research interests are the provision, analysis, and management of quality of service guarantees in communication networks. A particular focus has been on network calculus and its applications.

Jiahui Guo (S'13) received the B.S. degree in electrical engineering from Tsinghua University, Beijing, China, in 2011 and the M.S. degree in electrical engineering from the University of Tennessee, Knoxville, TN, USA, in 2014, where he is currently pursuing the Ph.D. degree in power systems.

His current research interests include wide-area power system monitoring, situational awareness, and data analytics.

Yilu Liu (S'88–M'89–SM'99–F'04) received the B.S. degree in electrical engineering from Xi'an Jiaotong University, Xi'an, China, in 1982, and the M.S. and Ph.D. degrees in electrical eNovel trend of "l" shape in PD pattern to judge the appropriate crucial moment of replacing cast-resin current transformerngineering from Ohio State University, Columbus, OH, USA, in 1986 and 1989, respectively.

Currently, she is a Governors Chair Professor at the University of Tennessee - Knoxville (UTK), Knoxville, TN, USA, and Oak Ridge National Laboratory (ORNL), Oak Ridge, TN, USA. She leads the effort to establish a nationwide power frequency dynamic monitoring network (FNET), which is now operated at UTK and ORNL as GridEye (fnetpublic.utk.edu). Her current research interests include power system wide-area monitoring and control, large interconnection level dynamic simulations, electromagnetic transient analysis, and power transformer modeling and diagnosis.

Prof. Liu is a Member of the National Academy of Engineering.